Australasian Transport Research Forum 2022 Proceedings
28-30 September, Adelaide, Australia
Publication website: http://www.atrf.info

Multivariate Time-varying Kalman Filter Approach for Cycle-based Maximum Queue Length Estimation

A.Wanuji.N.Abewickrema[1], Mehmet Yildirimoglu[1], Jiwon Kim[1]

[1] School of Civil Engineering, Faculty of Engineering, Architecture and Information Technology, The university of Queensland, St Lucia, Queensland 4072, Australia

Email for correspondence: w.abewickrema@uq.edu.au

1. Introduction

Real-time queue length at signalized intersections has long been acknowledged as an essential parameter for traffic management and control. The literature on real-time queue length estimation comprises two distinct domains based on the underlying theory. First domain of models is based on the analysis of cumulative traffic input-output to a signal link based on the conservation law that was first proposed by (Webster, 1958) and later improved by many other researchers. Although these models are conceptually quite simple, there are several important limitations. Specifically, cumulative input-output models can capture the queue length accurately only when the rear end of the queue does not exceed the detector site. Further, this category of models cannot be utilized for the estimation of queue lengths that appear due to over-saturated traffic conditions. The second model domain is based on the propagation of traffic shockwaves. The shockwave model may successfully explain both the temporal and spatial dimensions of a complex queuing process. However, this model includes significant assumptions regarding the propagation of shockwaves and require vehicle arrivals data, which cannot be collected on most roadway sections.

Various model-based approaches exist in the literature for estimating the length of a queue in real time utilizing different data sources that offer either Eulerian or Lagrangian measurements. Nevertheless, with the increasing availability of high-resolution event-based detector data recently, consideration was given to exploiting such data to recover the event history of a traffic signal and to provide a foundation for analyzing the relationship between signal phase changes and traffic flow during the queue formation and discharging processes (Liu et al., 2009; Wu et al., 2010; Wu & Liu, 2011). Specifically, such high-resolution data exposes "break points" that detect traffic flow pattern variations (traffic state changes). Of particular interest for our study, (Liu et al., 2009) suggested a breakpoint-based queue length estimating approach for queue-over-detector (QOD) scenarios, where queues grow beyond the advance detectors. The critical step in their method was to identify the breakpoints indicating the transition of traffic states during queuing process at the detector location, situated sufficiently away from the intersection stop line. The maximum queue length was then estimated by reconstructing shockwave profiles in accordance with the theory of shockwaves. The limitations when applying the breakpoint-based model to estimate lane specific, cycle-based maximum queue lengths are identified as:

i. The incorrect identification of break points resulting in estimation inaccuracies.
ii. The vehicle detector must be positioned far enough from the intersection stop line
iii. Inability to perform sequentially in both under-saturated and over-saturated conditions

To overcome the above limitations, this paper presents a novel Kalman filter framework that can combine several measurement types in a time-varying way to estimate the cycle-based maximum queue length. This framework considers the measurement errors and uncertainties in the state variables (i.e., maximum queue length).

2. Methodology

2.1.Breakpoint Identification and deterministic models

Traffic states are defined by the vehicle flow, q (veh/h) and the corresponding density, k (veh/km). The transition of traffic states within each signal cycle can be depicted spatiotemporally using the traffic shockwave diagram, aligning with the signal phases of each cycle. The time at which traffic transitions from one state to another is defined as a "*break point*". If the n^{th} signal cycle is under-saturated (cycle condition 1 of Figure 1), three main break points named as break point A, B and C could be identified and if the n^{th} signal cycle is over-saturated (cycle condition 2 of Figure 1) another break point called break point D will appear instead of break point C. To distinguish each of the break points A, B, C, and D using 2s occupancy data, distinct threshold values were established. The time that point "A" appears (T_A) is the moment that the queuing shock wave V_1^n propagates upstream and crosses the loop detector site. Between T_r^n (start of red phase) and T_A, the vehicles pass the loop detector with the arrival traffic state (q_a^n, k_a^n) while between T_A and T_B, no vehicle can pass the loop detector because of the jam traffic condition $(0, k_j)$. In this study, based on our observations, if there is an occupancy change from less than 100% to 100% occupancy and if the occupancy value is kept at 100% for more than 4 s (2 of 2-seconds time intervals) within red phase, it can be categorized as break point "A". Point B represents the time (T_B) at which the discharge shockwave, V_2 reaches the detector location. Between effective green start T_g^n and, T_B the traffic state over the detector is $(0, k_j)$; after T_B, vehicles are discharged at saturation flow rate and traffic state changes to (q_m, k_m). Based on our observations, if the occupancy remains 100% at least for two consecutive time intervals and then drops to a lower value than 100% occupancy within green phase, it can be categorized as a "B" break point. Identification of point "C" is the most challenging step. Point C indicates the time (T_C) when the rear end of queue passes the detector. Before point C appears, vehicles discharge at the saturation flow rate at the location of loop detector, i.e., the traffic state is (q_m, k_m). After the departure shockwave V_3^n propagates to the detector location, the traffic state changes to (q_a^n, k_a^n). Based on our observations, having 0% occupancy for at least two consecutive 2 seconds time intervals (4s) in a green phase assure the appearance of point C. In over-saturated cycles, due to the residual queue occupying the detector site the departure

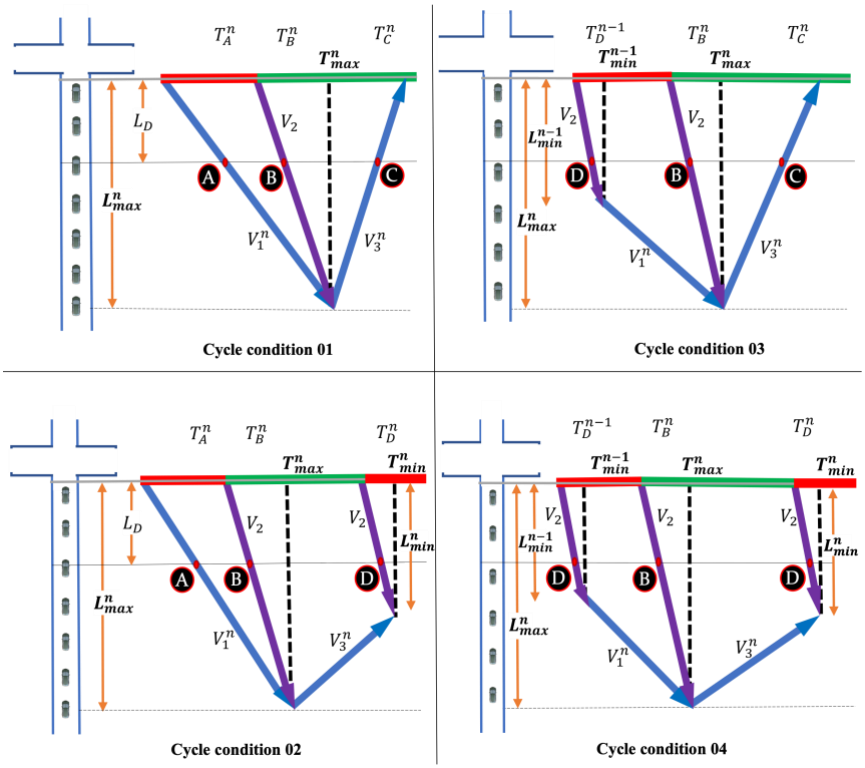

Figure 1. Possible signal cycle conditions

wave V_3^n will not be crossing the detector site and thus breakpoint C will be unobservable at the detector site. Instead, a breakpoint "D" will appear which defines the traffic state transition from saturation state (q_m, k_m) back to jam state (0, k_j). Breakpoint D appears when the queue discharging at a saturation flow rate is unable to clear during the green phase and becomes stationary. Breakpoint D was identified through the occupancy change happening at a beginning of a signal cycle from a value between 20% -80% occupancy (corresponding to the saturation flow rate according to the simulation results) to 100% occupancy and continues for at least 2 consecutive time steps when a point C is not detected in the previous signal cycle. It should be noted that the threshold values of point A and point D are very similar and that could result in misidentification of point A as D and vice versa. Hence, it is important to investigate the appearance of point C in the $(n-1)^{th}$ signal cycle to confirm whether the identified point is point A or point D at the beginning of n^{th} signal cycle. Four possible signal cycle conditions were determined when studying the observed break points described above (please see Figure 1). The cycle conditions indicate all possible traffic state transitions in signal cycle n that can occur in relation to the conditions in the previous cycle $(n-1)$ and the next cycle $(n+1)$, as described below.

Cycle condition 01: Both $(n-1)^{th}$ cycle and n^{th} cycle is under-saturated, hence the beginning of the n^{th} cycle is not impacted by a residual queue nor the end of n^{th} cycle (beginning of $(n+1)^{th}$ cycle). Therefore, breakpoints A, B and C appears sequentially.

Cycle condition 02: $(n-1)^{th}$ cycle is under-saturated but n^{th} cycle is over-saturated, hence the beginning of the n^{th} cycle is not impacted by a residual queue but the end of n^{th} cycle (beginning of $(n+1)^{th}$ cycle). Therefore, breakpoints A, B and D appears sequentially.

Cycle condition 03: $(n-1)^{th}$ cycle is over-saturated but n^{th} cycle is under-saturated, hence the beginning of the n^{th} cycle is impacted by a residual queue but not the end of n^{th} cycle (beginning of $(n+1)^{th}$ cycle). Therefore, breakpoints D, B and C appears sequentially.

Cycle condition 04: Both $(n-1)^{th}$ cycle and n^{th} cycle is over-saturated, hence the beginning of the n^{th} cycle and the end of n^{th} cycle (beginning of $(n+1)^{th}$ cycle) is impacted by a residual queue. Therefore, breakpoints D, B and D appears sequentially.

We developed four models (eq. 1-5) to estimate the cycle-based maximum queue length (L_{max}^n) based on the identified breakpoints A, B, C, and D and the signal cycle conditions. The cycle-based maximum queue length (L_{max}^n) is the vertical distance between the intersection stop line and the place where three shockwaves (V_1^n, V_2 and V_3^n) intersect. Hence, using any of these two waves, the coordinates of the intersection point of these three waves can be determined.

$$\boldsymbol{L_{max}^n = \frac{q_{BC}^n}{k_j} + L_D} \quad (1)$$

$$L_{max}^n = L_D + (T_C - T_B)^n \Big/ \left(\frac{1}{V_2} + \frac{1}{V_3^n}\right) \quad (2)$$

$$L_{max}^n = L_D + (T_A - T_B)^n \Big/ \left(\frac{1}{V_2} - \frac{1}{V_1^n}\right) \quad (3)$$

$$L_{max}^n = \frac{V_1^n V_2 \left(T_D^n - T_B^n\right)}{\left(V_1^n - V_2\right)} + L_{min}^{n-1} \quad (4)$$

$$\text{Where, } L_{min}^{n-1} = \frac{V_2\left[L_{max}^{n-1} + V_2 T_{max}^{n-1} - V_3^{n-1} T_r^n\right]}{\left(V_2 + V_3^{n-1}\right)} \quad (5)$$

2.2. Design and implementation of multivariate time-varying Kalman filter

We relied only on readings collected from loop detectors when detecting traffic state changes. Specifically in the case of high-resolution detector data, it can cause significant inaccuracies in flow and occupancy measurements. To overcome this problem, this study proposes a novel approach that employs the four deterministic models introduced in the previous section as measurement models in a multivariate Kalman filter framework. In this application, we consider the cycle-based maximum queue length (L_{max}^{n}) and the cycle-based minimum queue length (L_{min}^{n}) as the unknown or hidden state variables. The four models (eq. 1-5) are incorporated as linear measurement models which describes the relationship between the state variables (L_{max}^{n} and L_{min}^{n}) and measurements. The Kalman filter is often interpreted as two different phases: "Predict" and "Update." The predict phase uses the state estimate from the previous time step (a priori) to produce an estimate of the state at the current time step. In the update phase, the current a priori prediction is combined with current observation information to refine the state estimate. This improved estimate is termed the a posteriori state estimate.

The standard Kalman filter model assumes the true state at time t is evolved from the state at $(t-1)$ according to a process model of:

$$x_t = F_t x_{t-1} + B_t u_t + \omega_t \quad (6)$$

Where:

- F_t is the state transition model which is applied to the previous state $(t-1)$
- B_t is the control input model which is applied to the control vector u_t
- ω_t is the process noise which is assumed to be drawn from a zero-mean multivariate normal distribution, N, with covariance, Q_t: $\omega_t \sim \mathrm{N}(0, Q_t)$

At time t an observation (or measurement) z_t of the true state x_t is made according to a measurement model of:

$$z_t = H_t x_t + v_t \quad (7)$$

Where:

- H_t is the observation model which maps the true state space into the observed space
- v_t is the observation noise which is assumed to be zero-mean Gaussian white noise with covariance R_t: $v_t \sim \mathrm{N}(0, R_t)$

When considering L_{max}^{n} and L_{min}^{n} as the state variables, the process model should describe how the state variable evolves over time. The behavior of L_{max}^{n} and L_{min}^{n} is indeed a complex process that is challenging to model when a fixed sampling interval is considered. Therefore, a simple random walk model is assumed to be the process model that defines the time evolvement of the state variables, L_{max}^{n} and L_{min}^{n} with a fixed sampling interval equal to the signal cycle length. It should be noted that for the design simplicity of the Kalman filter, L_D, which is the distance from the stop line to the detector site was incorporated into the state variable matrix as a constant. In our case study, L_D =35m. Therefore, the process model of this system is defined as:

$$L_{max}^{n} = L_{max}^{n-1} + e_{1-1} \quad (8)$$

$$L_D = L_D\ (constant) \quad (9)$$

$$L_{min}^{n} = L_{min}^{n-1} + e_{1-2} \quad (10)$$

Where:

- n is the time step which is equal to the signal cycle length (150 seconds)
- e_{1-1}, e_{1-2} are white process noises $\sim N(0, Q)$

The four deterministic models (equations 1, 2, 3, and 4) generated in the preceding section were used as measurement models for the Kalman filter. By arranging the measurements to be on the left side of the equations, the model equations are reorganized as follows.

$$q_{BC}^{n} = k_j * L_{max}^{n} - k_j * L_D + e_2 \quad (11)$$

$$(\boldsymbol{T_C - T_B})^{\boldsymbol{n}} = \left(\frac{1}{V_2} + \frac{1}{V_3^n}\right) * \boldsymbol{L_{max}^{n}} - \left(\frac{1}{V_2} + \frac{1}{V_3^n}\right) * \boldsymbol{L_D} + \boldsymbol{e_3} \quad (12)$$

$$(\boldsymbol{T_A - T_B})^{\boldsymbol{n}} = \left(\frac{1}{V_2} - \frac{1}{V_1^n}\right) * \boldsymbol{L_{max}^{n}} - \left(\frac{1}{V_2} - \frac{1}{V_1^n}\right) * \boldsymbol{L_D} + \boldsymbol{e_4} \quad (13)$$

$$(\boldsymbol{T_D - T_B})^{\boldsymbol{n}} = \left(\frac{1}{V_2} - \frac{1}{V_1^n}\right) * \boldsymbol{L_{max}^{n}} - \left(\frac{1}{V_2} - \frac{1}{V_1^n}\right) * \boldsymbol{L_{min}^{n-1}} + \boldsymbol{e_5} \quad (14)$$

In the proposed Kalman filter framework, all 4 models (eq. 1-4) are considered together as measurement models thus it is called a multivariate Kalman filter. Hence, the measurements matrix (z_t) and the measurement function matrix (H_t) can be written as follows for the multivariate-time varying Kalman filter with the state variable matrix, X. R_t is the measurement covariance matrix.

$$X = \begin{bmatrix} L_{max}^{n} \\ L_D \\ L_{min}^{n} \end{bmatrix} \qquad z_t = \begin{bmatrix} q_{BC}^{n} \\ (T_C - T_B)^n \\ (T_A - T_B)^n \\ (T_D - T_B)^n \end{bmatrix}$$

$$H_t = \begin{bmatrix} k_j & -k_j & 0 \\ \left(\frac{1}{V_2} - \frac{1}{V_1^n}\right) & -\left(\frac{1}{V_2} - \frac{1}{V_1^n}\right) & 0 \\ \left(\frac{1}{V_2} + \frac{1}{V_3^n}\right) & -\left(\frac{1}{V_2} + \frac{1}{V_3^n}\right) & 0 \\ \left(\frac{1}{V_2} - \frac{1}{V_1^n}\right) & 0 & -\left(\frac{1}{V_2} - \frac{1}{V_1^n}\right) \end{bmatrix} \qquad R_t = \begin{bmatrix} R_{e2} & 0 & 0 & 0 \\ 0 & R_{e3} & 0 & 0 \\ 0 & 0 & R_{e4} & 0 \\ 0 & 0 & 0 & R_{e5} \end{bmatrix}$$

R_{e2}, R_{e3}, R_{e4} are the covariances of $e_2, e_3,$ and e_4 corresponding to the measurement errors. A significant difference exists in measurement model 2, 3 and 4 (eq. 12-14) compared to measurement model 1 (eq. 11). The measurement function (H_t) is a constant in eq.11 which is k_j, the jam density of the road segment while in eq. 12-14, V_1^n and V_3^n parameters are embedded which are time dependent. As the V_1^n and V_3^n shockwave speeds rely on the arrival traffic flow of each signal cycle and hence these two parameters should be updated during each epoch of the estimation. In our algorithm, these two parameters are updated during each epoch which makes the filter a "time varying" filter. Thus, the final algorithm developed under this study is called multivariate time-varying Kalman filter.

3. Simulation results and analysis

Results generated through a 3-hour simulation for the mixed traffic condition (contains all cycle conditions) is shown in Figure 2 below. The signal cycles belonging to the respective cycle conditions described in Figure 1 are depicted in different colors and labeled 1,2, 3, and 4 corresponding to the respective cycle condition in Figure 2. Figure 2 also indicates the performance of the rule-based models for comparison.

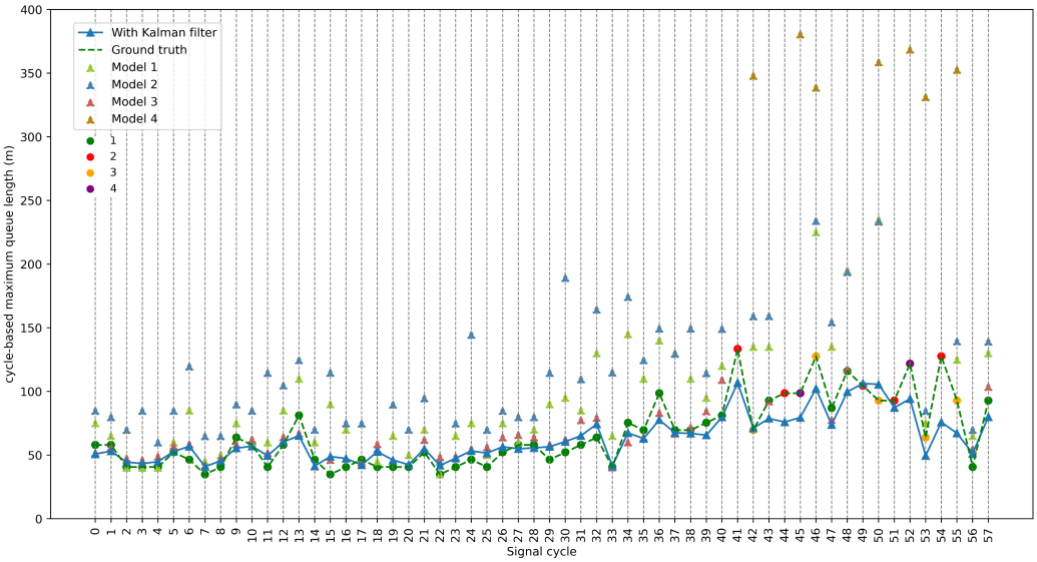

Figure 2. Performance of the Multivariate time-varying Kalman filter

The results of the mixed traffic condition indicates that the Kalman filter framework performs with a significant accuracy resulting in a MAPE value of 14.27 with acceptable estimation for the over-saturated cycles. The covariance values, P, Q *and* R (act as hyper parameters of the Kalman filter) were selected through engineering intuition considering the real performance of the dynamic system.

4. Conclusion

The Kalman filter estimator performs significantly well in all defined cycle conditions. As a future step, we will validate the methodology with real world data obtained via STREAMS platform available for Brisbane. Additionally, advanced prediction models instead of the random walk model will be further investigated as an expansion to the current study. Further, a prior optimization algorithm to choose the optimal hyper parameter values of the Kalman filter will increase the adaptability of the algorithm in different real-world applications.

5. Acknowledgement

This is an Australian Research Council Linkage Project named “Real-time Analytics on Urban Trajectory Data for Road Traffic Management” in collaboration with Queensland Department of Transport and Main Roads (TMR) and Transmax Pty. Ltd. Further, this research is funded by iMOVE CRC and supported by the Cooperative Research Centres program, an Australian Government initiative.

6. References

Liu, H., He, R., Zhang, K., & Li, J. (2009). A neural network model for travel time prediction. *Proceedings - 2009 IEEE International Conference on Intelligent Computing and Intelligent Systems, ICIS 2009*, *1*, 752–756. https://doi.org/10.1109/ICICISYS.2009.5358018

Webster. (1958). Traffic Signals Webster. *Road Research Technical Paper*, *39*, 1–44. https://trid.trb.org/view.aspx?id=113579

Wu, X., & Liu, H. X. (2011). A shockwave profile model for traffic flow on congested urban arterials. *Transportation Research Part B: Methodological*, *45*(10), 1768–1786. https://doi.org/https://doi.org/10.1016/j.trb.2011.07.013

Wu, X., Liu, H. X., & Gettman, D. (2010). Identification of oversaturated intersections using high-resolution traffic signal data. *Transportation Research Part C: Emerging Technologies*, *18*(4), 626–638. https://doi.org/https://doi.org/10.1016/j.trc.2010.01.003